

Photoresponsive Supramolecular Systems: Self-Assembly of Azodibenzoic Acid Linear Tapes and Cyclic Tetramers

Felaniaina Rakotonradany, M. A. Whitehead, Anne-Marie Lebuis, and Hanadi F. Sleiman*^[a]

Abstract: A new strategy to effect photoinduced control over molecular self-assembly is reported. This strategy uses the reversible *trans*–*cis* photoisomerization of a novel azobenzene system, where the *trans*- and *cis*-forms self-assemble into dramatically different higher-order structures. The *trans*-azo-

benzene form of this molecule associates into infinite hydrogen-bonded linear

Keywords: azobenzene • hydrogen bonds • photochromism • self-assembly • supramolecular chemistry

tapes, while the *cis*-azobenzene form undergoes hydrogen-bonded self-assembly into cyclic tetramers. This results in a second level of association, where the *cis*-hydrogen-bonded supramolecular cycles ultimately form long, rod-like aggregates through stacking interactions.

Introduction

Molecular self-assembly has recently emerged as one of the most efficient methods to create new materials with controlled physical and chemical properties.^[1] In particular, hydrogen-bonded self-assembly has generated an impressive range of structures, such as helices,^[1] linear tapes,^[1, 2] cyclic arrays^[1, 2d, 3] and three-dimensional objects.^[1, 4] An especially attractive goal is to use external stimuli, such as electrical, chemical or optical signals to control the self-assembly process.^[1–11] In particular, photoswitchable units have been incorporated in a variety of supramolecular systems,^[5–11] such as peptides,^[5] DNA,^[6] dendrimers,^[7] molecular hosts^[8] as well as macromolecular and liquid crystalline structures.^[9, 10] These systems have almost exclusively relied on the photoswitching of a molecule between two distinct states,^[5–8] or on using the reversible photoisomerization of a chromophore to pattern a surrounding polymer or liquid crystal matrix.^[9, 10]

We here report a new strategy to effect photochemical control over molecular self-assembly, by using photoresponsive azobenzene units **1** and **2** as *supramolecular* building blocks (Scheme 1). This results in the light-driven switching of

a material between two dramatically different nanoscale morphologies.^[11] The *trans*-azobenzene form of these molecules **1** associates into infinite hydrogen-bonded *linear tapes*, while the *cis*-azobenzene form **2** undergoes hydrogen-bonded self-assembly into cyclic tetramers, which then further associate to form long, rod-like aggregates.

In the design of molecule **1**, the photoswitchable azobenzene unit is incorporated in the main chain, and two hydrogen bonding carboxylic acids are *para* to the N=N linkage. Dicarboxylic acids, such as isophthalic and terephthalic acid derivatives have been shown to associate into discrete hexameric rosettes and linear tapes, respectively.^[3a,b] The azobenzene units in molecule **1** can undergo a reversible *trans*–*cis* photoisomerization.^[12] In the *trans*-isomer **1**, the two carboxylic groups are expected to be aligned, and they can thus undergo hydrogen-bonding self-assembly into linear aggregates. On the other hand, in the photogenerated *cis*-form **2**, the carboxylic acids are expected to be oriented in a near perpendicular fashion, thus they can self-assemble into cyclic structures (Scheme 1). Building block **1** also incorporates two long alkoxy chains *ortho* to the azo group, in order to sterically favor the formation of discrete, cyclic structures once converted to the *cis*-form **2**.^[3]

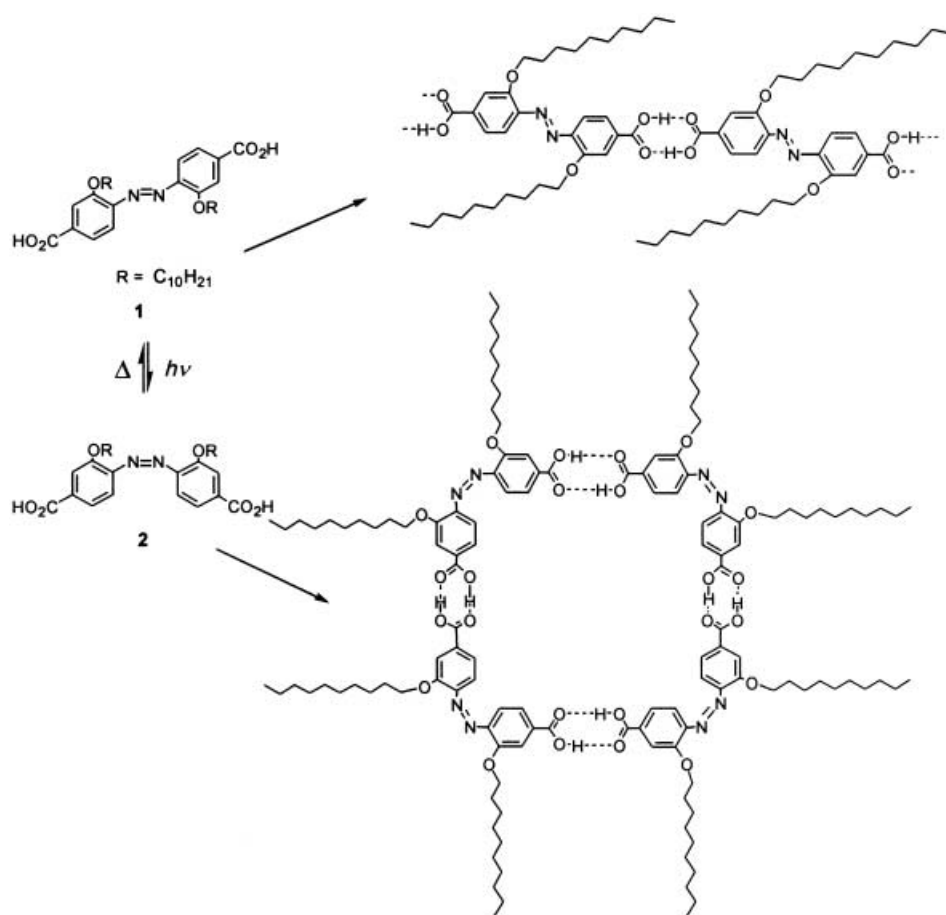
Results and Discussion

Theoretical calculations: To validate the above assumptions, we first investigated the geometry of *cis-p*-azodibenzoic acid as a model compound by semiempirical PM3,^[13a,b] density functional theory (B3LYP^[13c]/6-31G*), as well as ab initio (HF/6-31G*) molecular orbital calculations.^[13] These consis-

[a] Prof. H. F. Sleiman, F. Rakotonradany, Prof. M. A. Whitehead, Dr. A.-M. Lebuis

Department of Chemistry, McGill University
801 Sherbrooke Street West
Montréal Québec H3A 2K6 (Canada)
Fax: (+1)514-398-3797
E-mail: hanadi.sleiman@mcgill.ca

Supporting information for this article is available on the WWW under <http://www.chemeurj.org/> or from the author.



Scheme 1. Hydrogen bond self-assembly of *trans*-**1** and *cis*-**2** azodibenzoic acid.

tently showed similar C–N=N bond angles for this building block, and an orientation of 82° between the carboxylic acid groups. We then proceeded to perform PM3 calculations, using the unsubstituted *p*-azodibenzoic acid, as well as *o*-bis(methoxy)azodibenzoic acid as model compounds, in order to estimate the most stable supramolecular structures from *trans*-**1** and *cis*-**2**. PM3 enthalpies and Gibbs free energies of reaction at 298 K were calculated for the formation of open and closed oligomers from monomeric *trans*- and *cis*-azodibenzoic acids (Table 1).^[14]

These calculations indicated that the *trans*-azodibenzoic acid self-assembles most favorably into linear tapes (Figure 1), while *cis*-azodibenzoic acid is most likely to form cyclic structures (Figure 2).^[15] Comparison of the closed aggregates indicated that the cyclic tetramer shown in Figure 2 is thermodynamically more stable than both the pentameric and hexameric rosettes^[16] (see Table 1). These calculations also suggested that the formation of closed structures from azodibenzoic acid trimers might be difficult. Consequently, as expected from our design, PM3 calculations predict that *trans*-azodibenzoic acid forms oligomeric linear tapes, whereas *cis*-azodibenzoic acid **2** associates into cyclic structures; this suggests that the self-assembly of **1** can be reversibly photo-induced between dramatically different structures. Notably this study is one of a few examples of the use of semiempirical calculations to fully optimize a supramolecular assembly.^[17]

Synthesis and self-assembly of *trans*-azodibenzoic acid **1**:

Scheme 2 outlines the synthesis of **1** from 3-hydroxy-4-nitrobenzoic acid (**3**). Carboxylic acid **3** was first protected in acidic media to give ester **4**, which was then treated with a stoichiometric amount of 1-bromodecane under mild basic conditions. The resulting ether **5** was deprotected under reflux in 1:1 KOH/MeOH, then reduced using zinc dust under basic conditions. The desired azodibenzoic acid **1** was isolated by chromatography of the corresponding methyl ester, followed by hydrolysis under basic conditions.^[14]

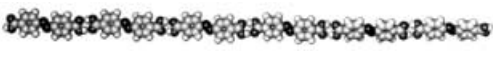





We first studied the hydrogen-bond self-assembly behavior of *trans*-azodibenzoic acid **1**. Vapor pressure osmometry (VPO) measurements were carried out in CH_2Cl_2 , using benzil ($M_w = 210$) as the molecular weight standard.^[18] The calculated y intercept of the plot of VPO molecular weight versus concentration was found to match the origin, and the calculated association constants of

dimer, trimer, tetramer, and so on were nearly equal.^[14] This indicates that **1** does not form discrete aggregates, but rather oligomeric linear chains. Single crystals of *trans*-**1** were grown by evaporation of a DMF solution, and the X-ray structure is shown in Figure 3.^[19] Diacid **1** does indeed form an extended hydrogen-bonded network of linear tapes, confirming the PM3 calculations and the VPO results. In addition, these tapes pack together through their long alkyl substituents to form infinite parallel sheets (Figure 3b and c). This high crystallinity of the *trans*-**1** monomer is also observed in its powder diffraction (XRD) pattern (see Figure 5a).

Reversible photoisomerization of *trans*-azodibenzoic acid **1** to the *cis*-form **2**:

The propensity of *trans*-**1** to undergo reversible photoisomerization was then examined by UV/Vis and ^1H NMR spectroscopy. Irradiation of samples of *trans*-**1** at $\lambda > 300$ nm results in a decrease in the two UV/Vis absorption maxima at 321 and 387 nm, with an isobestic point around 286 nm, and the appearance of a new peak at 250 nm corresponding to *cis*-**2** (Figure 4). In $[\text{D}_6]\text{DMSO}$, this photoisomerization results in distinct ^1H NMR signals for *trans*-**1** and *cis*-**2**, and a 1:1.3 *trans*–*cis* photostationary state can be reached after 2 h of irradiation. Kinetic studies were carried out on the thermal conversion of *cis*-azodibenzoic acid **2** to *trans*-**1**, using both UV/Vis and ^1H NMR in DMSO ,^[14] and an activation enthalpy $\Delta H^\ddagger = 84.9 \pm 2.5$ kJ mol $^{-1}$ and entropy

Table 1. PM3 standard enthalpies and Gibbs free energy of the self-assembly as a function of the hydrogen-bonded aggregate formed with the *trans*- and the *cis*-azodibenzoic acids at 298 K. These energies were obtained by subtracting the cumulated energies of the *n* monomers involved in the self-assembly of the compound from the energy of the formed complex.

	Hydrogen-bonded aggregates		ΔH_f^0 [kcal mol ⁻¹]	ΔG_f^0 [kcal mol ⁻¹]
<i>trans</i> - 1 linear tape		<i>n</i> = 6	-24.46	-11.24
<i>cis</i> - 2 linear tape		<i>n</i> = 6	-39.55	31.25
<i>cis</i> - 2 trimer		<i>n</i> = 3	-15.27	12.71
<i>cis</i> - 2 cyclic tetramer		<i>n</i> = 4	-30.87	8.62
<i>cis</i> - 2 cyclic pentamer		<i>n</i> = 5	-37.42	15.34
<i>cis</i> - 2 cyclic hexamer		<i>n</i> = 6	-43.72	19.49

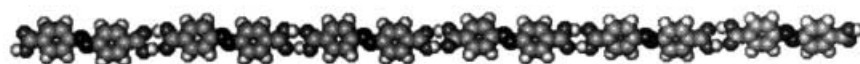


Figure 1. PM3 optimized geometry of a linear hexameric tape formed from *trans*-azodibenzoic acid.

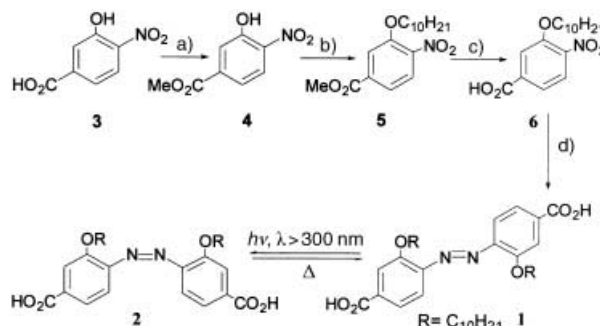


Figure 2. PM3 optimized geometry of the square formed from *cis*-azodibenzoic acid.

$\Delta S^\ddagger = -72.8 \pm 8.0 \text{ J mol}^{-1} \text{ K}^{-1}$ were obtained. These results were similar to previously obtained parameters for *ortho*-alkyl azobenzenes.^[20] The conversion of *cis*-**2** to *trans*-**1** was complete in 1 h at 70 °C. These studies thus demonstrate the

ready formation of *cis*-**2** via photochemical isomerization of **1**, and its facile thermal conversion to *trans*-**1**.

In DMSO, *trans*-**1** and *cis*-**2** are expected to exist in their monomeric form, therefore the kinetics involve the isomerization of monomeric *cis*-**2** to monomeric *trans*-**1**. However, in a non-competitive solvent such as chloroform, *trans*-**1** and *cis*-**2** should associate into hydrogen-bonded structures. Thus, the kinetics in chloroform should reflect the interconversion between self-assembled supramolecular structures of *cis*-**2** and *trans*-**1**, and are expected to differ for this reaction from the results obtained in CH₃OH or DMSO. The photoisomerization behavior ($\lambda > 300 \text{ nm}$) of *cis*-**2** to *trans*-**1** in CDCl₃ was compared with that in [D₆]DMSO and CD₃OD, using ¹H NMR spectroscopy at a range of temperatures (20 to -30 °C). While the photostationary state was rapidly reached upon photolysis of *cis*-**2** in all solvents even at low temperatures (ca. 5 min), the *cis*-*trans* photoisomerization rate was nearly double in [D₆]DMSO and [D₄]methanol than in CDCl₃. This is consistent with the need for dissociation of the hydrogen-bonded supramolecular structure formed by *cis*-**2** in CDCl₃, prior to its reisomerization to *trans*-**1**.



Scheme 2. Synthesis of 2,2'-bis(decyloxy)-4,4'-azodibenzoic acid **1**. a) Conc. H₂SO₄, MeOH, reflux, 48 h; b) 1-C₁₀H₂₁Br, anhydrous K₂CO₃, DMF, N₂ atmosphere, 80 °C, 24 h; c) KOH pellets, 1:1 MeOH/H₂O, reflux, 4 h; d) Zn dust (1.6 equiv), 30% aq. NaOH, 24 h; Zn dust (1.4 equiv), water, 3 d.

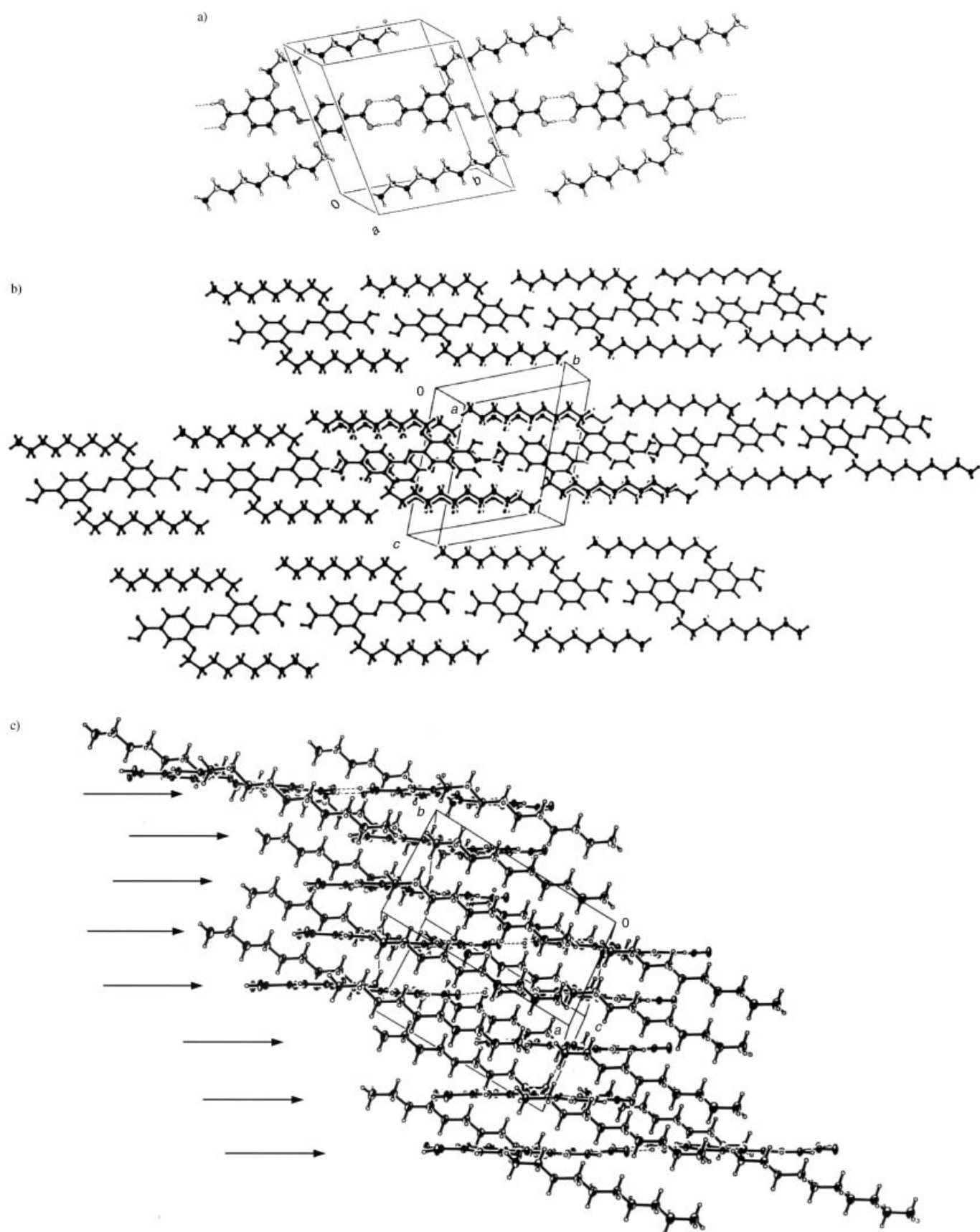


Figure 3. a) X-ray single crystal data showing the hydrogen-bonded tapes formed by *trans*-1. b) Sheets formed upon aggregation of these tapes (top view). c) Sheets formed from these tapes (side view). The arrows indicate the planes defined by the sheets.

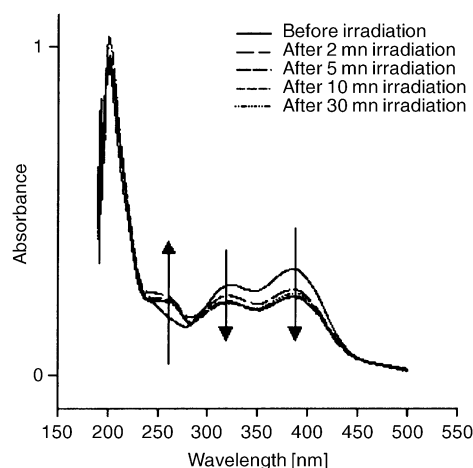


Figure 4. UV/Vis absorption spectrum recorded during the UV irradiation ($\lambda > 300$ nm) of a 3.44×10^{-5} M solution of *trans-1* in methanol.

Kinetic studies were carried out on the thermal conversion of *cis*-azobenzene **2** to *trans-1* in CHCl_3 , using UV/Vis and ^1H NMR spectroscopy.^[14] The enthalpy of activation obtained was higher in CHCl_3 ($\Delta H^\ddagger = 97.4 \pm 4.2 \text{ kJ mol}^{-1}$) than DMSO ($\Delta H^\ddagger = 84.9 \pm 2.5 \text{ kJ mol}^{-1}$), and the entropy of activation ($\Delta S^\ddagger = -15.9 \pm 13.7 \text{ J mol}^{-1} \text{ K}^{-1}$) was more positive in CHCl_3 than DMSO ($\Delta S^\ddagger = -72.8 \pm 8.0 \text{ J mol}^{-1} \text{ K}^{-1}$). This data is consistent with an additional contribution to the enthalpy of activation of the *cis*–*trans* isomerization, which involves dissociation of the *cis-2* hydrogen-bonded supramolecular structure. Furthermore, the larger entropy of activation is consistent with the presence of a higher degree of order in the supramolecular structure of *cis-2* in CHCl_3 than in the monomeric structure of **2** in DMSO. Consequently, the kinetic behavior observed in chloroform for the *cis*–*trans* isomerization is consistent with the formation of higher-order supramolecular structures from *cis-2*, and their thermal and photochemical switching to the *trans-1* linear tapes (see above).

cis-Azobenzene **2** can be isolated from photoirradiated samples of *trans-1* using reverse-phase HPLC,^[14] and its stability (up to 2 d in the dark at 20°C and two weeks at 4°C) allowed its full characterization. As will be shown, the self-assembly behavior of *cis-2* is radically different from *trans-1*. *cis-2* is significantly more soluble in non-polar solvents (e.g., CH_2Cl_2) than *trans-1*. ^1H NMR spectra of **2** (CD_2Cl_2) taken at a range of concentrations, show symmetrical azobenzene peaks. These results are consistent with the formation of a discrete cyclic structure, rather than oligomeric aggregates from this molecule. Examination of the aromatic region upon dilution (from a saturated 3.0 mM solution to 0.2 mM), showed a small shift of ≈ 0.01 ppm for these peaks. This shift was accompanied by a peak sharpening, which suggests the existence of π – π stacking interactions in solution.^[21]

Vapor pressure osmometry (VPO) studies were carried out on solutions of **2** in CH_2Cl_2 . In order to determine the molecular weight of the hydrogen-bonded structure formed by **2**, two molecular weight standards were used for this experiment, and the experiment was repeated using two different osmometers.^[14] In all cases, the plots of VPO

molecular weight versus concentration showed clear y intercepts corresponding to $M_n = 2210$ using benzil ($\Delta = 1.2\%$) and $M_n = 2317$ using polystyrene ($\Delta = 0.1\%$), consistent with the formation of a tetramer ($M_n = 2328$) in solution.^[14] In addition, ESI-MS enabled the detection of a tetrameric structure at m/z 2330.^[14]

X-ray powder diffraction spectra were obtained for *cis-2*, and showed a dramatically different supramolecular structure for this isomer than for *trans-1* (Figure 5b). In contrast to the sharp peaks obtained for **1**, the spectrum of **2** features one main broad peak at 14.0° , followed by three less intense peaks at 24.0 , 25.7 , and 27.0° .^[22a]

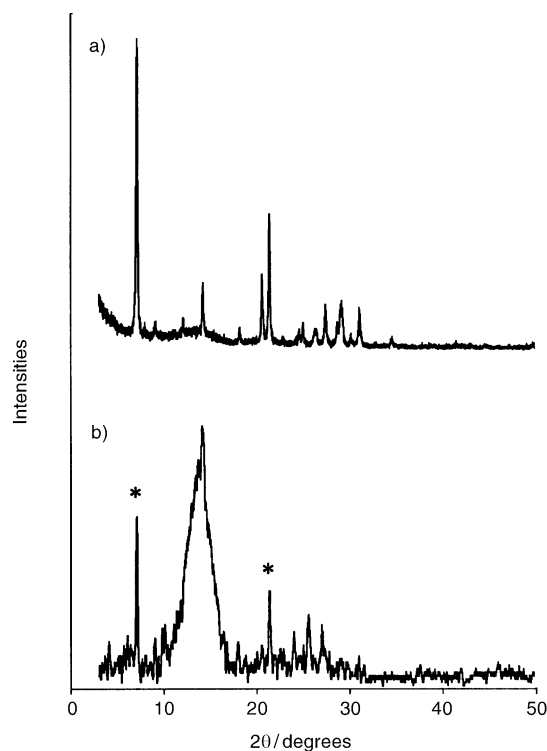


Figure 5. a) X-ray diffraction (XRD) pattern for *trans-1*. b) XRD pattern for *cis-2*. The asterisks mark the presence of *trans-1* impurities.

Applying Scherrer's equation to the width at half-height of the main diffraction peak^[22b,c] gave a crystal dimension of 3.6 ± 0.2 nm for this solid. This distance is in good agreement with the expected diameter for a *cis-2* cyclic tetramer (4.2 nm).^[23] Thus ^1H NMR spectroscopy, vapor pressure osmometry, ESI-MS, X-ray powder diffraction studies, as well as theoretical PM3 calculations are all consistent with the self-assembly of *cis-2* into discrete cyclic tetramers, in contrast with the oligomeric linear tapes obtained from *trans-1*.^[24]

Transmission electron microscopy and dynamic light scattering studies: Transmission electron microscopy (TEM) studies of *trans-1* and *cis-2* allowed direct visualization of the large differences in their self-assembly behavior. Interestingly, these studies also revealed a second level of self-organization of these molecules. Figures 6 and 7 show transmission electron micrographs of replicas prepared from dispersions of *trans-1* and *cis-2* in 1,2-dichloroethane or by direct deposition onto a

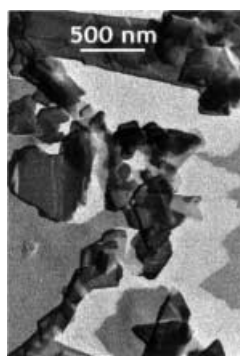


Figure 6. TEM of a replica for *trans-1*.

carbon-coated grid.^[25] Large, sheet-like aggregates are observed for *trans-1* (Figure 6), consistent with the ordered arrangement of stacked linear tapes from this molecule (Figure 3). On the other hand, the TEM of samples of *cis-2* showed the formation of dramatically different supramolecular structures. In contrast with *trans-1*, periodic arrays of elongated aggregates, with length as great as 170 nm, arise from the *cis-2* isomer (Figure 7). In some cases, these structures aggregate into large bundles of 23 nm in diameter and 430 nm in length (Figure 7d). The outer hydrodynamic diameter was measured as ≈ 3.9 nm, in agreement with the estimated diameter of the self-assembled supramolecular cycles of *cis-2* (4.2 nm), and as already shown by our XRD, VPO and PM3 studies (see above). This diameter was observed on more than 10 different, freshly purified samples of *cis-2*, and for various deposition conditions (direct deposition and replica methods, see Experimental Section).^[25] This result suggests further organization of the supramolecular cycles from *cis-2* through π - π stacking and/or alkyl-alkyl interactions. Among the possible higher-order arrangements consistent with these observations, we have considered the two structures shown in Figures 7e and f. Rod-like structures would arise as a result of stacking interactions along the normal to the macrocycle plane (Figure 7e). Preliminary molecular mechanics MM⁺ and PM3 calculations showed that favorable π - π stacking of these *cis*-azodibenzoic acid supramolecular cycles can result into unidimensional, rod-like structures, when the aromatic rings are slightly rotated (ca. 30°) relative to the normal of the macrocycle plane, and the interplanar distances are shorter than ≈ 4.5 Å.^[14, 26] On the other hand, side-by-side, lateral arrangement of these macrocycles with their rings parallel to the normal of the macrocycle plane can also lead to structures with high aspect ratio (Figure 7f). We are currently using both spectroscopic techniques (e.g., solid-state NMR) and theoretical studies to determine

whether the *cis-2* macrocycles pack into either of these modes, or into other intermediate higher-order arrangements.

Dynamic light scattering (DLS) studies were carried out for *cis-2* in 1,2-dichloroethane at scattering angles of 45, 90, and 135°, and confirmed the presence of these elongated aggregates in solution.^[27] The hydrodynamic diameters obtained for these angles were significantly different from one angle to the other, for example, 745 nm at 45° and 566 nm at 135°, clearly demonstrating the presence of elongated, rather than spherical *cis-2* aggregates in solution. In addition, changes in concentration led to diameters varying from 282–746 nm at 1.0 g L⁻¹ and 565–746 nm at 2.5 g L⁻¹, consistent with the formation of longer structures at higher concentration.^[14] Another set of DLS experiments was carried out for solutions of *cis-2*, which were cooled to 4 °C for 2 d. These measurements indicate that much longer, non-spherical aggregates with hydrodynamic diameters ranging from 3090.0 to 4572.5 nm were formed. Thus, the photochemically formed *cis-2* undergoes self-assembly into elongated aggregates both in solution (DLS) and in the solid state (TEM).

Conclusion

We have shown that the self-assembly of azodibenzoic acids **1** and **2** can be reversibly photoswitched between two dramati-

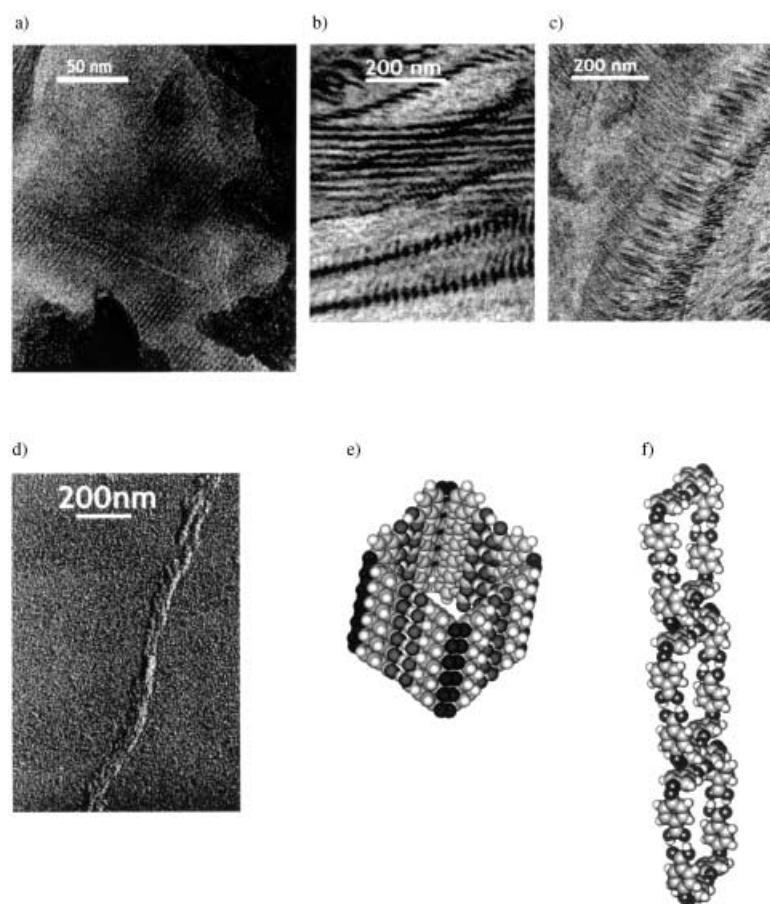


Figure 7. a) TEM of directly deposited films of *cis-2*. b), c) and d) TEM of replicas of *cis-2*. e) and f) Representations of possible packing modes (alkyl chains are omitted for clarity).

ically different supramolecular structures. On a first level, photoirradiation triggers the *trans* → *cis* azobenzene isomerization, which changes the self-assembly of these molecules from linear tapes in the *trans*-form, to discrete cyclic structures in the *cis*-form. On a second level, these *cis*-azobenzene cyclic structures self-organize into elongated aggregates through stacking interactions. Overall, a primary photochemical event of the *trans*–*cis* isomerization has been considerably amplified using supramolecular self-assembly. We are currently investigating the use of this novel strategy for the creation of reversibly photopatterned surfaces. In addition, efforts towards further stabilization of the *cis*-azobenzene form by increasing the number of hydrogen bonding interactions are currently underway.

Experimental Section

Materials: 3-Hydroxy-4-nitrobenzoic acid was purchased from the Aldrich Chemical Co. Methyl 3-hydroxy-4-nitrobenzoate (**3**) was synthesized according to the reported procedure.^[28] The structures of the intermediates and the final products were confirmed by FTIR and NMR spectroscopy, high-resolution and low-resolution MS, and elemental analysis.

Equipment: ¹H and ¹³C NMR spectra were acquired on a Varian Mercury 400 and 500 MHz spectrometers. Infrared spectra were acquired on a Bruker IFS-48 FTIR spectrometer (solution, resolution: 2 cm⁻¹). UV/Vis spectra were measured on a Varian CARY 1 UV/Vis spectrophotometer equipped with a Peltier-temperature controller. Preparative HPLC was carried out using a Hewlett-Packard model equipped with a semipreparative Zorbax 300 SB-C18 9.4 mm × 25 cm reverse phase column. Transmission electron microscopy (TEM) was conducted on a JEOL-2000 FX instrument by using the replica and the direct deposition methods. Vapor pressure osmometry (VPO) measurements were carried out in dichloromethane using a Model 233 Molecular Weight Apparatus by Wescan Instruments, Inc. A second set of measurements was carried out in dichloromethane using Vapro 5520-model vapor pressure osmometer equipped with AC-066 Head for 0–3200 mmol kg⁻¹ range manufactured by Wescor. Electrospray ionization (ESI) was performed using a Finnigan SSO7000 (ThermoFinnigan) or a Quattro II triple quadrupole (Micromass, Manchester, UK) mass spectrometer equipped with a syringe pump (Harvard Apparatus). X-Ray diffraction data were collected using a Siemens D-5000 diffractometer, consisting of a step scanner equipped with a 1.2 kW cobalt tube ($\lambda = 1.78897 \text{ \AA}$) coupled to a silicon detector.

Methyl 3-decyloxy-4-nitrobenzoate (4): 3-Hydroxy-4-nitrobenzoic acid methyl ester (**3**; 2.00 g, 10.15 mmol), 1-bromodecane (2.1 mL, 10.15 mmol), anhydrous K₂CO₃ (4.20 g, 30.45 mmol), and dry DMF (26 mL) were purged with nitrogen. The reaction mixture was heated to 80 °C under nitrogen for 24 h. After cooling to room temperature, the heterogenous mixture was poured into ice-cooled water, and the resulting precipitate **4** was filtered, washed with water and dried (3.27 g, 96%). ¹H NMR ([D₆]acetone): $\delta = 7.91$ (d, 1H), 7.83 (s, 1H), 7.72 (d, 1H), 4.28 (t, 2H), 3.93 (s, 3H), 1.83 (m, 2H), 1.51–1.31 (m, 14H), 0.88 (t, 3H); ¹³C NMR (CDCl₃): $\delta = 165.27, 151.94, 142.47, 134.63, 125.14, 121.02, 115.37, 69.90, 52.78, 31.84, 29.48, 29.47, 29.26, 29.19, 28.76, 25.74, 22.64, 14.08$; EI-MS: *m/z*: calcd for C₁₈H₂₇NO₅: 337.4; found: 337.0.

3-Decyloxy-4-nitrobenzoic acid (5): Methyl 3-decyloxy-4-nitrobenzoate (**4**; 1.44 g, 4.27 mmol) and KOH pellets (287.5 g, 5.12 mmol) were heated to reflux in a 1:1 MeOH/H₂O mixture (4 mL) for 4 h. The disappearance of the ester was checked by thin-layer chromatography (silica gel, dichloromethane). The reaction mixture was cooled using an ice-water bath, and concentrated HCl (≈ 1.5 mL) was added dropwise. The resulting precipitate was filtered, washed with water and air-dried (1.27 g, 93%). ¹H NMR ([D₆]DMSO): $\delta = 7.92$ (d, 1H), 7.73 (d, 1H), 7.61 (dd, 1H), 4.20 (t, 2H), 1.70 (m, 2H), 1.38–1.23 (m, 14H), 0.84 (t, 3H); ¹³C NMR (CDCl₃): $\delta = 169.21, 151.94, 143.09, 133.70, 125.21, 121.72, 115.82, 69.98, 31.86, 29.75, 29.55, 29.47, 29.03, 26.02, 22.92, 22.59, 14.34$; FTIR (CHCl₃): $\tilde{\nu} = 2976$ (C–H), 1717.4 (C=O), 1529.3 (N=O); EI-MS: *m/z*: calcd for C₁₇H₂₅NO₅: 323.4; found:

323.5; elemental analysis calcd (%) for C₁₇H₂₅NO₅·2KCl: C 43.21, H 5.33, N 2.96; found: C 43.63, H 5.17, N 2.90.

trans-2,2'-Bis(decyloxy)-4,4'-azodibenzoic acid (1): 3-Decyloxy-4-nitrobenzoic acid (**5**; 1.073 g, 3.32 mmol) was heated to 80 °C in the presence of Zn dust (347.5 mg, 5.31 mmol), in 30% aqueous NaOH (15.55 mL). After 23 h, the reaction mixture was diluted with water (62 mL), and Zn dust was added (303.9 mg, 4.65 mmol). The reaction mixture was heated to 80–85 °C for 3 d, and then cooled and filtered. The orange solution was acidified with glacial acetic acid. The obtained precipitate was filtered and washed with water (3 × 50 mL) and a minimum of ethanol (≈ 20 mL). The solid was dissolved in dilute aqueous ammonia, the solution was acidified with dilute hydrochloric acid and heated to gentle reflux for 5 min. The resulting solid was filtered, washed repeatedly with water and ethanol, and dried. The crude (476 mg) contains a mixture of azoxy-, azo- and hydrazobenzene derivatives. These were methylated with diazomethane. The methyl esters were separated by silica gel chromatography with dichloromethane. The isolated methyl azodibenzoate (284.7 mg, 0.47 mmol) was then hydrolyzed by refluxing for 4 h in a solution of KOH (pellets, 109.6 mg, 1.96 mmol) in 1:1 EtOH/H₂O (12 mL). Acidification with hydrochloric acid at 0 °C, filtration and drying gave **1** as yellow crystals (267.7 mg, 28%). ¹H NMR ([D₆]DMSO): $\delta = 7.71$ (d, 2H), 7.58 (dd, 2H), 7.47 (dd, 2H), 4.22 (t, 4H), 1.78 (m, 4H), 1.45–1.19 (m, 28H), 0.80 (t, 6H); ¹³C NMR ([D₄]methanol): $\delta = 174.33, 157.45, 145.39, 142.94, 122.74, 117.42, 116.50, 70.66, 33.07, 30.80, 30.66, 30.46, 30.34, 27.25, 23.74, 14.47$. FTIR (CH₂Cl₂): $\tilde{\nu} = 3677, 3595$ (O–H), 2976, 2915 (C–H), 1604 (C=O); FAB-MS (positive mode): *m/z*: calcd for 583.7; found: 583.0; MALDI-TOF MS: *m/z*: calcd for C₃₄H₅₀N₂O₆·Li⁺: 589.7; found: 589.0; elemental analysis calcd (%) for C₃₄H₅₀N₂O₆: C 70.07, H 8.65, N 4.81; found: C 69.67, H 8.94, N 4.45.

cis-2,2'-Bis(decyloxy)-4,4'-azodibenzoic acid (2): An NMR tube filled with a solution of azodibenzoic acid **1** (7 mg, 0.012 mmol) in [D₆]DMSO (0.7 mL) was fitted inside a photochemical reactor equipped with a 450 W Hanovia lamp, for which a Pyrex sleeve was used to cut-off the wavelengths below 300 nm. The disappearance of the *trans*-isomer, and appearance of *cis*-isomer were monitored by ¹H NMR. A 1:1.3 *trans/cis* photostationary state (¹H NMR) was reached after 1 h. The reverse *cis*–*trans* thermal isomerisation in solution is quantitative after 2–3 d in the dark at room temperature, and upon heating at 70 °C for 1 h in [D₆]DMSO. The *cis*-isomer was isolated by reverse phase HPLC. A 30 min gradient of 90:10 to 100:0 MeOH/H₂O (+0.06% TFA) was used as the mobile phase. The UV detector was set at 286 nm, which corresponds to the isobestic point observed when the *trans*-isomer is irradiated in methanol. The collected fractions were immediately stored in the dark at low temperature (+4 °C) before solvent evaporation in order to avoid thermal reisomerisation. ¹H NMR ([D₆]DMSO): $\delta = 7.42$ (d, 2H), 7.35 (dd, 2H), 6.62 (d, 2H), 3.96 (t, 4H), 1.65 (m, 4H), 1.45–1.17 (m, 28H), 0.83 (t, 6H); FAB-MS (positive mode): *m/z*: calcd for 583.7; found: 583.0.

Thermal cis–trans reisomerisation kinetics by ¹H NMR: An NMR tube of irradiated azodibenzoic acid (5 mg, 0.008 mmol) in [D₆]DMSO (0.7 mL) was maintained at temperatures between 25 and 60 °C. The kinetics of the reaction were followed by monitoring the ¹H NMR signal of the methylenic protons α to the ether oxygen (triplets between 3.5–4.5 ppm, where *trans*-**1** appears at 4.25 ppm and *cis*-**2** at 3.99 ppm).

Thermal cis–trans reisomerisation kinetics by UV/Vis: A solution of irradiated azodibenzoic acid (1 mg, 0.002 mmol) in DMSO (100 mL) was maintained at temperatures between 25 and 60 °C. The kinetics of the reaction were followed by monitoring the increase in absorbance at 315 nm. A solution of *cis*-**2** azodibenzoic acid (1 mg, 0.002 mmol) in CHCl₃ (100 mL) was maintained at temperatures between 20 and 45 °C. The kinetics of the reaction were followed by monitoring the increase in absorbance at 309 nm.

Vapor pressure osmometry (VPO) measurements: A total of eight different stock solutions of *cis*-azodibenzoic acid at concentrations ranging from 2 to 12 g L⁻¹ were prepared in dichloromethane. 30 μ L of solution were injected into the osmometer chamber. After temperature equilibration (5 min), the voltage was recorded in mV. Three independent measurements were made at each concentration, and the experiments were duplicated. A calibration curve was generated using benzil ($M = 210.23$) and polystyrene ($M = 2100$) as molecular weight standards under the same conditions. Average molecular weight of studied aggregates were calculated using Equation (1):

$$M_{\text{Wunknown}} \times \lim_{C \rightarrow 0} \frac{VPO_{\text{unknown}}}{C_{\text{unknown}}} = M_{\text{Wstandard}} \times \lim_{C \rightarrow 0} \frac{VPO_{\text{standard}}}{C_{\text{standard}}} \quad (1)$$

Using a different instrument (see above), a total of six different stock solutions of *cis*- and *trans*-azodibenzoic acid were prepared in dichloromethane (higher solubility was observed for the *cis*-isomer than for the *trans*-isomer). 10 μL of solution were placed into the osmometer sample holder. After temperature equilibration (75 s), osmolality was recorded in mmol kg^{-1} . Five independent measurements were made at each concentration, and the experiments were duplicated. A calibration curve was generated using benzil ($M = 210.23$) as the standard under the same conditions and the molecular weights were obtained.

Electrospray ionization mass spectrometry (ESI) measurements: A solution of *cis*-**2** in dichloromethane (or chloroform), to which were added a few μL methanol, was infused at a flow rate of $5 \mu\text{L min}^{-1}$ for molecular weight determination. The spectrometer was programmed to scan for the negative product ions to give monomer, dimer, trimer and tetramer between m/z 100 and m/z 2500 with a spray voltage of 3.5 kV and capillary heater at 200°C , trimer with a spray voltage of 4.0 kV and capillary heater at 150°C and tetramer with a spray voltage of 3.5 kV and capillary heater at 150°C .

A solution of *cis*-**2** in chloroform onto which were added a few μL of 5–30 mM Et_3N was directly infused into the mass spectrometer, which was configured for negative product ion analysis and used with the spray voltage set to 3.5 kV, source temperature 50°C , sample infusion rate $5 \mu\text{L min}^{-1}$. The spectrometer was programmed to scan for the product ions from m/z 400 to 2800 in multichannel acquisition mode (MCA) showing m/z for monomer, dimer, trimer and tetramer/ Et_3N complex.

Sample preparation for TEM measurements by the replica method: A solution of *cis*-**2** or *trans*-azodibenzoic acid **1** was prepared by dissolving the sample in 1,2-dichloroethane into a vial wrapped in aluminum foil at room temperature, and deposited on a freshly cleaved mica sheet. 7–9 μL of solution were transferred via pipet onto the mica leaf. After allowing the solvent to evaporate for 1–2 min, the mica sample was placed inside a high-vacuum Edwards Carbon coater equipped with Pt-C and C-guns. The replicas were prepared by successive evaporation of Pt-C at a 15° angle then carbon at a 90° angle on the air-dried sample. Each gun was consecutively turned on for about 10–15 s, starting with the Pt-C gun. The replica was detached from the mica surface by floating the thin Pt/C film on distilled water, transferred onto a 400 mesh TEM copper grid and dried overnight on filter paper, before observation under the microscope. On the micrographs, the Pt-C is seen as dark gray and the carbon as light gray. The size of the Pt-covered substrate agree with the size of the shadow. For the replicas, the error estimate on the measurements is ± 1 nm.

Sample preparation for TEM measurements by the direct method: A solution of *cis*- (**2**) or *trans*-azodibenzoic acid **1** was prepared by dissolving the sample in 1,2-dichloroethane into a vial wrapped in aluminum foil at room temperature. A carbon-coated 400 mesh copper grid, prewashed with chloroform for 12 h was dipped into the solution for approximately 5 min then dried on a filter paper.

X-ray powder diffraction (XRD) measurements: X-ray diffraction patterns were acquired for 2θ values ranging from 3 to 50° for *trans*-**1** and *cis*-**2** azodibenzoic acid powders. Diffraction patterns for the *cis*-isomers were acquired on freshly chromatographed and vacuum-dried samples over 2–3 d. Despite these precautions, some thermal reisoimerization to the *trans* isomer was observed by X-ray diffraction.

Dynamic light scattering (DLS) measurements: Dynamic light scattering measurements were carried out using a 532 nm laser equipped photomultiplier detector. The autocorrelation functions were acquired for θ values of 45 , 90 and 135° for prefiltered solutions of *trans*-**1** and *cis*-**2** azodibenzoic acid in 1,2-dichloroethane. The wavelength of the laser source corresponds to an absorption minimum for the *cis*-azodibenzoic acid **2** in this solvent. Data acquisition was carried out at 20°C and within a few hours to prevent any thermal reisoimerization of the *cis*-isomer. Inverse Laplace transforms of the data were performed using Provencher's FORTRAN program CONTIN,^[30] diffusion coefficients were determined from the slope of the relaxation frequencies (Γ) vs q^2 . Assuming a spherical behaviour for the particles and using the translational coefficient D_{T} and the Stokes–Einstein equation, the hydrodynamic diameters are calculated for each scattering angle.

Theoretical calculations: Optimizations of the azodibenzoic acid supramolecular assemblies were performed using the PM3 semiempirical molecular orbital theory,^[17b,c] which is less computationally expensive than ab initio or density functional methods. In addition, density-functional theory (DFT) B3LYP/6-31G* and ab initio HF/6-31G* calculations were performed on the *cis*-*p*-azodibenzoic acid monomer to confirm the geometry obtained using PM3.

The geometry of the *trans*- and *cis*-monomers were optimized using PM3 until an RMS gradient of 0.01 was reached. After this optimization, another monomer was added and the hydrogen-bonded structure energy was minimized. This monomer addition-optimization sequence was repeated up to the hexameric compound. The hydrogen-bonded geometry and the total heat of formation were extracted for each optimized species. Standard Gibbs free energies were obtained for each optimized structure by vibrational analysis.

Geometry optimizations used the PM3 method contained in the Gaussian98W^[30] program package. PM3 frequencies were obtained from Gaussian98W. Frequencies were scaled using the default settings (Scaling factor = 0.8929).

Calculations for the packing of the *cis*-**2** azodibenzoic acid tetramers were performed using the molecular mechanics MM⁺ applied to the Ring Packing Scan (RPS) method. This method consists in a rigid scan of the total energies of the stacked macrocycles while changing the distances between 3.5 – 6.0 Å along the z axis and between 0.0 – 2.0 Å along the x axis. The obtained minimum geometry was then optimized using PM3.

Acknowledgement

This work was supported by NSERC (Canada), CFI (Canada), FCAR (Québec) and the Research Corporation (USA). H.F.S. is a Cottrell Scholar of the Research Corporation. The authors gratefully acknowledge Prof. R. St. J. Manley (PAPRICAN) for the loan of the 450W Hanovia UV/Vis photochemical reactor, Prof. A. D. Chapman (Concordia University) for the loan of the Vapro 5520-model vapor pressure osmometer, Prof. G. Bazuin (U. Laval) for the loan of the Model 233 tonometer and Ms. R. Plésu (U. Laval) for technical assistance for the use of the tonometer, J. Wright (Concordia University) and D. Dennie (McGill University) for the acquisition of the electrospray ionization mass spectra.

- [1] a) J.-M. Lehn, *Supramolecular Chemistry: Concepts and Perspectives*, VCH, Weinheim, **1995**; b) G. M. Whitesides, E. E. Simanek, J. P. Mathias, C. T. Seto, D. N. Chin, M. Mammen, D. M. Gordon, *Acc. Chem. Res.* **1995**, *28*, 37–44; c) J. S. Lindsey, *New J. Chem.* **1991**, *15*, 153–180; d) D. S. Lawrence, T. Jiang, M. Levett, *Chem. Rev.* **1995**, *95*, 2229–2260; e) S. Leininger, B. Olenyuk, P. J. Stang, *Chem. Rev.* **2000**, *100*, 853–907.
- [2] a) J.-M. Lehn, M. Mascal, A. DeCian, J. Fischer, *J. Chem. Soc. Chem. Commun.* **1990**, 479–481; b) J. A. Zerkowski, C. T. Seto, D. A. Wierda, G. M. Whitesides, *J. Am. Chem. Soc.* **1990**, *112*, 9025–9026.
- [3] a) J. Yang, J.-L. Marendaz, S. J. Geib, A. D. Hamilton, *Tetrahedron Lett.* **1994**, *35*, 3665–3668; b) A. Zafar, J. Yang, S. J. Geib, A. D. Hamilton, *Tetrahedron Lett.* **1996**, *37*, 2327–2330; c) M. Mammen, E. E. Simanek, G. M. Whitesides, *J. Am. Chem. Soc.* **1996**, *118*, 12614–12623; d) M. Mascal, N. M. Hext, R. Warmuth, J. R. Arnall-Culliford, M. H. Moore, J. P. Turkenburg, *J. Org. Chem.* **1999**, *64*, 8479–8484; e) C. M. Drain, X. Shi, T. Milic, F. Nifiatis, *Chem. Commun.* **2001**, 287–288; f) S. V. Kolotuchin, S. C. Zimmerman, *J. Am. Chem. Soc.* **1998**, *120*, 9092–9093; g) H. Fenniri, B.-L. Deng, A. E. Ribbe, K. Hallenga, J. Jacob, P. Thiyagarajan, *Proc. Natl. Acad. Sci.* **2002**, *99*, 6487–6492.
- [4] a) T. Kusukawa, M. Fujita, *J. Am. Chem. Soc.* **1999**, *121*, 1397–1397; b) K. S. Kim, S. B. Suh, J. C. Kim, B. H. Hong, E. C. Lee, S. Yun, P. Tarakeswar, J. Y. Lee, Y. Kim, H. Ihm, H. G. Kim, J. W. Lee, J. K. Kim, H. M. Lee, D. Kim, C. Cui, S. J. Youn, H. Y. Chung, H. S. Choi, C.-W. Lee, S. J. Cho, S. Jeong, J.-H. Cho, *J. Am. Chem. Soc.* **2002**, *124*, 14268–14279.
- [5] a) M. S. Vollmer, T. D. Clark, C. Steinem, M. R. Ghadiri, *Angew. Chem.* **1999**, *111*, 1703–1706; *Angew. Chem. Int. Ed.* **1999**, *38*, 1598–

- 1601; b) D. T. Bong, T. D. Clark, J. R. Ganja, M. R. Ghadiri, *Angew. Chem.* **2001**, *113*, 1016–1041; *Angew. Chem. Int. Ed.* **2001**, *40*, 988–1011.
- [6] H. Asanuma, T. Ito, T. Yoshida, X. Liang, M. Komiyama, *Angew. Chem.* **1999**, *111*, 2547–2549; *Angew. Chem. Int. Ed.* **1999**, *38*, 2393–2395.
- [7] D. M. Junge, D. V. McGrath, *J. Am. Chem. Soc.* **1999**, *121*, 4912–4913.
- [8] a) S. Tsuchiya, *J. Am. Chem. Soc.* **1999**, *121*, 48–53; b) M. Takeuchi, S. Shinkai, *J. Chem. Soc. Perkin Trans. 2* **1998**, 847–852.
- [9] a) K. Ichimura, *Chem. Rev.* **2000**, *100*, 1847–1873; b) C. Ruslim, K. Ichimura, *Macromolecules* **1999**, *32*, 4254–4263; c) H.-K. Lee, K. Doi, H. Harada, O. Tsutsumi, A. Kanazawa, T. Shiono, T. Ikeda, *J. Phys. Chem. B* **2000**, *104*, 7023–7028.
- [10] a) S. Kawata, Y. Kawata, *Chem. Rev.* **2000**, *100*, 1777–1788; b) A. Nathanson, P. Rochon, *Can. J. Chem.* **2001**, *79*, 1093–1100; c) *Holographic Data Storage* (Eds.: H. J. Coufal, D. Psaltis, G. T. Sincerbox), Springer, Berlin, Heidelberg, **2000**.
- [11] a) The control of gelation behavior has been reported with hydrogen bonding dithienylcyclopentenes: L. N. Lucas, J. van Esch, R. M. Kellogg, B. L. Feringa, *Chem. Commun.* **2001**, 759–760; b) T. Kawasaki, M. Tokuhira, N. Kimizuka, T. Kunitake, *J. Am. Chem. Soc.* **2001**, *123*, 6792–6800.
- [12] G. S. Hartley, *J. Chem. Soc.* **1938**, 633–642.
- [13] a) J. J. P. Stewart, *J. Comp. Chem.* **1989**, *10*, 209–220; b) J. J. P. Stewart, *J. Comp. Chem.* **1989**, *10*, 221–264; c) A. D. Becke, *J. Chem. Phys.* **1993**, *98*, 5648–5652; d) the C–N=N angle obtained by our PM3 calculations for *cis-p*-azodibenzoic acid (126.9°), *cis-o*-bis(methoxy)-*p*-azodibenzoic acid (127.2°), *cis-o*-bis(decyloxy)-*p*-azodibenzoic acid (127.8°) agrees with experimental X-ray results for *o*-substituted *cis*-azobenzene (126.4°) (see ref. [20]). The details of these calculations will be published elsewhere.
- [14] See Supporting Information.
- [15] Similar PM3 calculations were performed on hydrogen-bonded isophthalic acid aggregates. These theoretical studies agree with experimental evidence, showing that the unsubstituted isophthalic acid form tapes instead of rosettes (see ref. [3a,b]), thus validating our predictions.
- [16] Attempts to form cyclic *cis*-azodibenzoic acid trimers by using PM3 only yielded the open aggregates. A triangle was obtained from HF/STO-3G monomers, which were then assembled to form the desired structure, then optimized using PM3. This optimization gave a triangle with bent hydrogen-bonds, which were weaker than in the larger macrocycles and in the open aggregates.
- [17] Examples of supramolecular systems using semiempirical methods: a) R. Castro, M. J. Berardi, E. Cordova, M. O. de Olza, A. E. Kaifer, J. D. Evanseck, *J. Am. Chem. Soc.* **1996**, *118*, 10257–10268; b) S. Sharma, T. P. Radhakrishnan, *J. Phys. Chem. B* **2000**, *104*, 10191–10195; c) D. Quinonero, A. Frontera, S. Tomas, G. A. Suner, J. Morey, A. Costa, P. Ballester, P. M. Deya, *Theor. Chem. Acc.* **2000**, *104*, 50–66; d) K. S. Kim, S. B. Suh, J. C. Kim, B. H. Hong, E. C. Lee, S. Yun, P. Tarakeswar, J. Y. Lee, Y. Kim, H. Ihm, H. G. Kim, J. W. Lee, J. K. Kim, H. M. Lee, D. Kim, C. Cui, S. J. Youn, H. Y. Chung, H. S. Choi, C.-W. Lee, S. J. Cho, S. Jeong, J.-H. Cho, *J. Am. Chem. Soc.* **2002**, *124*, 14268–14279; e) A. Lützen, M. M. Hapke, J. Griep-Raming, D. Haase, W. Saak, *Angew. Chem.* **2002**, *114*, 2190–2194; *Angew. Chem. Int. Ed.* **2002**, *41*, 2086–2089.
- [18] E. E. Schrier, *J. Chem. Educ.* **1968**, *45*, 176–180.
- [19] a) X-ray crystal data for *trans*-azo **1**: Crystal dimensions: $0.69 \times 0.05 \times 0.03$ mm, unit cell: triclinic, $P\bar{1}$, $a = 8.3795(2)$, $b = 13.4914(3)$, $c = 15.1038(4)$ Å, $\alpha = 105.732(2)$, $\beta = 94.757(2)$, $\gamma = 91.273(2)^\circ$, $V = 1636.10(7)$ Å³, $\rho_{\text{calc}} = 1.183$ g cm⁻³, $\theta_{\text{max}} = 72.79$, $\text{CuK}\alpha$, $\lambda = 1.54178$ nm, collection method: phi scans, $T = 293$ K, 19813 measured reflections, 6258 independent reflections, 3029 observed reflections, maximum shift = 0.021, absorption correction type = multi scan, structure solution by direct method using SHELXS97, structure refinement using SHELXL96, 383 parameters, isotropic hydrogen atoms using defaults, $R1 = 0.0626$, $wR2 = 0.1750$, refinement against $|F^2|$. CCDC-184609 contains the supplementary crystallographic data for this paper. These data can be obtained free of charge via www.ccdc.cam.ac.uk/conts/retrieving.html (or from the Cambridge Crystallographic Data Centre, 12 Union Road, Cambridge CB2 1EZ, UK; (fax: (+44)1223-336-033; or e-mail: deposit@ccdc.cam.ac.uk); b) *International Tables for Crystallography*, Vol. C, Tables 4.2.6.8 and 6.1.1.4 Kluwer, Dordrecht, **1992**; c) SAINT Release 6.06, Integration Software for Single Crystal Data, Bruker AXS Inc., Madison, WI 53719-1173, **1999**; d) G. M. Sheldrick, SADABS, Bruker Area Detector Absorption Corrections. Bruker AXS Inc., Madison, WI 53719-1173, **1996**; e) SHELXTL Release 5.10, The Complete Software Package for Single Crystal Structure Determination, Bruker AXS Inc., Madison, WI 53719-1173, **1997**; f) SMART Release 5.059, Bruker Molecular Analysis Research Tool. Bruker AXS Inc., Madison, WI 53719-1173, **1999**; g) A. L. Spek, PLUTON Molecular Graphics Program, July 1995 version, University of Utrecht, Utrecht, Holland, **1995**; h) A. L. Spek, PLATON, Molecular Geometry Program, July 1995 version, University of Utrecht, Utrecht (Holland), (version 190499 at McGill), **1995**; i) XPREP Release 5.10, X-ray data Preparation and Reciprocal space, Exploration Program, Bruker AXS Inc., Madison, WI 53719-1173, **1997**.
- [20] N. J. Bunce, G. Ferguson, C. L. Forber, G. J. Stachnyk, *J. Org. Chem.* **1987**, *52*, 394–398.
- [21] A. S. Shetty, J. Zhang, J. S. Moore, *J. Am. Chem. Soc.* **1996**, *118*, 1019–1027.
- [22] a) When the diffraction pattern of *trans*-**1** was subtracted from the diffraction pattern of *cis*-**2**, the main diffraction peak appeared as one single peak. The peaks at 14.0, 24.0, 25.7 and 27.0° correspond to Bragg spacings of 0.73, 0.43, 0.40, and 0.38 nm, respectively. These dimensions may be related to the distance between two stacked cyclic tetramers of *cis*-**2**; b) B. D. Cullity, *Elements of X-Ray Diffraction*, Addison-Wesley, Reading, MA, **1978**; c) B.-Z. Zhan, M. A. White, K. N. Robertson, T. S. Cameron, M. Gharghoury, *Chem. Commun.* **2001**, 1176–1177.
- [23] This diameter was estimated from the PM3 optimized structure of the *cis*-azodibenzoic acid tetramer ($\varnothing = 2.31$ nm) onto which were superimposed four optimized decyloxy-substituted monomers. The distance between two opposite chain-ends was measured directly. See Supporting Information.
- [24] At very low concentrations ($c < 3$ g L⁻¹), the VPO data points lie slightly below the regression curves, suggesting the preponderance of monomeric species in such dilute solutions (See Supporting Information). However, at higher concentrations, the results are consistent with supramolecular tetramers.
- [25] On the micrographs, the Pt–C is seen as dark gray and the carbon as light gray. For the replicas, the error estimate on the measurements is ± 1 nm. (see Supporting Information for details). However, the *cis*-**2** isomer is expected to form hydrogen-bonded macrocycles in the solid state as reflected by our XRD and TEM results.
- [26] The total energy of stacked supramolecular structures was computed as a function of their inter-planar distance, the tilt of the aromatic rings with respect to the normal to the macrocycle plane, and the horizontal offset between the stacked macrocycles. The optimum structure obtained by using the MM⁺ force field was further optimized using PM3, leading to a very similar structure. Moreover, PM3 calculations on *cis-o*-bis(alkyl)azodibenzoic acid predict that the alkyl chains are able to adopt an orientation parallel to the azodibenzoic acid plane, thus enabling the hydrogen-bonding and stacking interactions to occur. As a result, PM3 and MM⁺ calculations show that the orientation of the aromatic rings in the macrocycle and the position of the alkoxy chains can favor the efficient stacking of these tetrameric macrocycles into rod-like morphologies. The details of these calculations will be published elsewhere.
- [27] See Experimental Section for details.
- [28] H. Zeng, R. S. Miller, R. A. II Flowers, B. Gong, *J. Am. Chem. Soc.* **2000**, *122*, 2635–2644.
- [29] a) S. W. Provencher, *Comput. Phys.* **1982**, *27*, 213–227; b) S. W. Provencher, *Comput. Phys.* **1982**, *27*, 229–242; c) K. S. Schmitz, *An Introduction to Dynamic Light Scattering by Macromolecules*, Academic Press Inc., San Diego, CA, **1990**.
- [30] *Gaussian 98W* (Revision A.7), M. J. Frisch, G. W. Trucks, H. B. Schlegel, G. E. Scuseria, M. A. Robb, J. R. Cheeseman, V. G. Zakrzewski, J. A. Montgomery, Jr., R. E. Stratmann, J. C. Burant, S. Dapprich, J. M. Millam, A. D. Daniels, K. N. Kudin, M. C. Strain, O. Farkas, J. Tomasi, V. Barone, M. Cossi, R. Cammi, B. Mennucci, C. Pomelli, C. Adamo, S. Clifford, J. Ochterski, G. A. Petersson, P. Y. Ayala, Q. Cui, K. Morokuma, D. K. Malick, A. D. Rabuck, K. Raghavachari, J. B. Foresman, J. Cioslowski, J. V. Ortiz, A. G. Baboul,

B. B. Stefanov, G. Liu, A. Liashenko, P. Piskorz, I. Komaromi, R. Gomperts, R. L. Martin, D. J. Fox, T. Keith, M. A. Al-Laham, C. Y. Peng, A. Nanayakkara, C. Gonzalez, M. Challacombe, P. M. W. Gill,

B. G. Johnson, W. Chen, M. W. Wong, J. L. Andres, M. Head-Gordon, E. S. Replogle, J. A. Pople, Gaussian, Inc., Pittsburgh PA, **1998**.

Received: February 20, 2003 [F4864]
